JOC Article

# MTO/$H_2O_2$/Pyrazole-Mediated N-Oxidation of *meso*-Tetraarylporphyrins and -chlorins, and S-Oxidation of a *meso*-Tetraaryldithiaporphyrin and -chlorin

Subhadeep Banerjee,[†] Matthias Zeller,[‡] and Christian Brückner*,[†]

*Department of Chemistry, University of Connecticut, Unit 3060, Storrs, Connecticut 06269-3060, and Department of Chemistry, Youngstown State University, One University Plaza, Youngstown, Ohio 44555-3663*

*c.bruckner@uconn.edu*

*Received March 11, 2009*



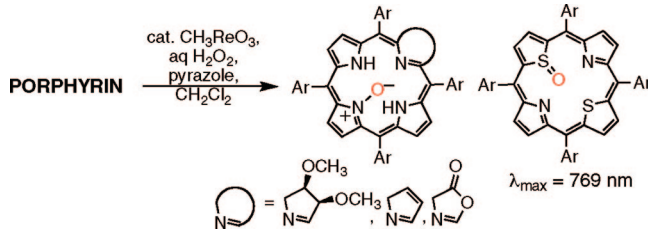


The methyltrioxorhenium (MTO)/pyrazole-mediated $H_2O_2$ oxidation of octaethylporphyrin and a number of *meso*-tetraarylporphyrins offers simple and good yielding access to the corresponding *N*-oxides, only few of which were prepared before. The crystal structure of a free base tetraarylporphyrin *N*-oxide demonstrates the degree to which the oxygenated pyrrole moiety is slanted with respect to the rest of the otherwise nearly planar macrocycle. The method is also suitable to the preparation of hitherto unknown chlorin *N*-oxides. Oxidation of *meso*-tetraphenyldithiaporphyrin and *meso*-tetraphenyldithiachlorin furnishes the corresponding novel *S*-oxides. The optical properties of the novel chromophores are described and rationalized.

## Introduction

Porphyrin *N*-oxides, such as octaethylporphyrin (OEP) *N*-oxide **1**, were first described in 1978 by Bonnett and Ridge.[1] Subsequently, it was shown that they could form metal complexes with Ni(II), Cu(II), Zn(II), Fe(III), and Tl(III) in which the oxygen bridges one N−M bond.[2−6] OEP *N*-oxide, in its free base or Ni(II) complex form, can be rearranged into a $\beta$-oxochlorin or its metal complex, respectively.[2,7] A tetraarylporphyrin *N*-oxide Fe(III) complex has been the source of an unusual ring-oxidized Fe(III) porphyrin complex.[8] The significance of the porphyrin *N*-oxide Fe(III) complexes with respect to possible heme degradation products or P-450 suicide reactions was also discussed.[1,3,9−12]

*N*-Oxide **1**, or its *meso*-tetraarylporphyrin analogues,[9,13] can be synthesized from their corresponding porphyrins by oxidation using either hypofluorous acid or organic acid peroxides, such as peracetic, permaleic acid, or *m*-CPBA.[2,3,14] Hypofluorous acid needs to be prepared fresh from gaseous fluorine and is po-

* To whom correspondence should be addressed: Fax: (+1) 860 486-2981. Phone: (+1) 860 486-2743.
[†] University of Connecticut.
[‡] Youngstown State University.

(1) Bonnett, R.; Ridge, R. J.; Appleton, E. H. *J. Chem. Soc., Chem. Commun.* **1978**, 310–311.
(2) Andrews, L. E.; Bonnett, R.; Ridge, R. J.; Appelman, E. H. *J. Chem. Soc., Perkin Trans. 1* **1983**, 103–107.
(3) Balch, A. L.; Chan, Y. W.; Olmstead, M.; Renner, M. W. *J. Am. Chem. Soc.* **1985**, *107*, 2393–2398.
(4) Balch, A. L.; Chan, Y.-W.; Olmstead, M. M. *J. Am. Chem. Soc.* **1985**, *107*, 6510–6514.
(5) Yang, F.-A.; Cho, K.-Y.; Chen, J.-H.; Wang, S.-S.; Tung, J.-Y.; Hsieh, H.-Y.; Liao, F.-L.; Lee, G.-H.; Hwang, L.-P.; Elango, S. *Polyhedron* **2004**, *25*, 2207–2214.
(6) Yang, F.-A.; Guo, C.-W.; Chen, Y.-J.; Chen, J.-H.; Wang, S.-S.; Tung, J.-Y.; Hwang, L.-P.; Elango, S. *Inorg. Chem.* **2007**, *46*, 578–585.
(7) Balch, A. L.; Chan, Y. W. *Inorg. Chim. Acta* **1986**, *115*, L45–L46.
(8) Tsurumaki, H.; Watanabe, Y.; Morishima, I. *J. Am. Chem. Soc.* **1993**, *115*, 11784–11788.
(9) Groves, J. T.; Watanabe, Y. *J. Am. Chem. Soc.* **1986**, *108*, 7836–7837.
(10) Groves, J. T.; Watanabe, Y. *J. Am. Chem. Soc.* **1988**, *110*, 8443–8452.
(11) Mizutani, Y.; Watanabe, Y.; Kitagawa, T. *J. Am. Chem. Soc.* **1994**, *116*, 3439–3441.
(12) Rachlewicz, K.; Latos-Grazynski, L. *Inorg. Chem.* **1996**, *35*, 1136–1147.
(13) Arasasingham, R. D.; Balch, A. L.; Olmstead, M. M.; Renner, M. W. *Inorg. Chem.* **1987**, *26*, 3562–3568.
(14) For an alterative, nongeneral photochemical pathway toward the Ti=O complex of a porphyrin *N*-oxide, see: (a) Hoshino, M.; Yamamoto, K.; Lillis, J. P.; Chijimatsu, T.; Uzawa, J. *Inorg. Chem.* **1993**, *32*, 5002–5003.

10.1021/jo9005443 CCC: $40.75 
Published on Web 05/07/2009

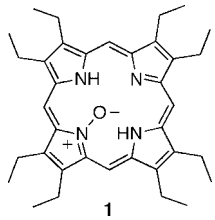

1

tentially explosive.[15] The peracid oxidation of *meso*-tetraarylporphyrins requires in some instances a large stoichiometric excess of peracids[9,13] and yet gives low yields for some derivatives (~5% for *meso*-4-pyridylporphyrins).[16] The best yielding peracid, permaleic acid, needs to be freshly prepared.

We are interested in the $\beta,\beta'$-bond manipulation of porphyrins. More generally, we search for novel methods to converting porphyrins to chlorins or pyrrole-modified porphyrins. As an entry point into the manipulation of the pyrrole moieties, we have largely relied on the stoichiometric $OsO_4$-mediated dihydroxylation of *meso*-tetraarylporphyrins,[17−20] but we are also searching for substitutes for the highly toxic and costly $OsO_4$. Over the past decade, the methyltrioxorhenium (MTO)/$H_2O_2$/base system has established itself as a superb epoxidation and dihydroxylation method.[21] Thus, we wanted to test whether MTO/$H_2O_2$/base could be used for the $\beta,\beta'$-epoxidation or dihydroxylation of porphyrins.

We describe here the results of this study. In short, MTO/$H_2O_2$/pyrazole proved unsuitable for the manipulation of a porphyrin $\beta,\beta'$-bond. Instead, we found these reagents to convert OEP and *meso*-tetraarylporphyrins to their *N*-oxides in good yields. Moreover, we successfully applied this reaction to *meso*-tetraphenyl-2,3-dimethoxychlorin, *meso*-tetraphenylporpholactone, and *meso*-tetraphenyldithiaporphyrin, generating the novel *N*- and *S*-oxides, respectively. We report here also on the effects *N*-oxidation has on the UV−vis spectra of the neutral and protonated chromophores.

## Results and Discussion

When we reacted OEP with the MTO/$H_2O_2$/pyrazole system under conditions reported to be optimized for olefin epoxidations (as opposed to dihydroxylation), that is, 25 mol % of MTO, a 20-fold stoichiometric excess of $H_2O_2$ (as a 30% aq solution), in the presence of pyrazole as base/ligand in $CH_2Cl_2$ at ambient temperature,[22] we observed its clean conversion into a product we identified as the corresponding *N*-oxide **1**.[2] Even over the course of reactions running up to 24 h, we observed no sign of any $\beta,\beta'$-bond reactivity. The yields using this method are around 57% (not taking into consideration that nearly 40% of the starting material that can be recovered). This compares to the reported yields using peracids which range, depending on the peracids used, from 26 to 68%.[2] Overall, we perceive the greatest advantage of the MTO/$H_2O_2$/pyrazole method toward the preparation of OEP *N*-oxide to be the use of readily available reagents, combined with its procedural simplicity.

**SCHEME 1. MTO/$H_2O_2$ Oxidation of *meso*-Tetraarylporphyrins**

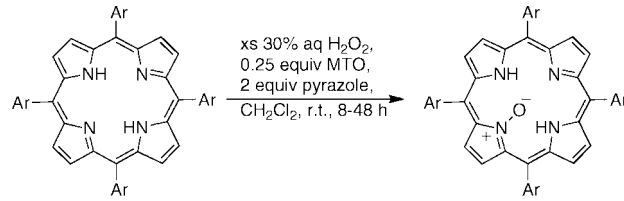


| | | |
|---|---|---|
| **2a** | Ar = Ph | **3a** (70%, 20% recovered **2a**) |
| **2b** | Ar = 4-Cl-Ph | **3b** (33-39%, 30% recovered **2b**) |
| **2c** | Ar = 4-$^t$Bu-Ph | **3c** (34%, 50% recovered **2c**) |
| **2d** | Ar = (3,4,5-MeO)Ph | **3d** (33-48%, 40% recovered **2d**) |
| **2e** | Ar = (2,3,4,5,6-F)Ph | **3e** (14%, 60% recovered **2e**) |

Like the peracid method, the MTO/$H_2O_2$/pyrazole reaction conditions could also be applied toward the *N*-oxidation of *meso*-tetraarylporphyrins (Scheme 1).[23] Thus, *meso*-tetraphenylporphyrin (**2a**) was converted in good average 61% yields (typical yields ranged from 50 to 80%) to the corresponding *N*-oxide **3a**, with ~20% of the starting material recovered. This compares very well to the reported 14.6% yield using permaleic acid.[23] A range of electron-rich (**2c** and **2d**) or electron-poor tetraarylporphyrins (**2b**, **2e**) are susceptible to these reaction conditions (Scheme 1). All products possessed the spectroscopic and analytical properties supporting their assigned structures. In all cases, we observed that very long reaction times or the use of much larger stoichiometric ratios of oxidant increased the formation of smaller amounts (<10%) of unidentified, high polarity degradation products. In neither case did we observe the formation of chlorin-like compounds (by UV−vis spectroscopy) that would indicate that a $\beta,\beta'$-functionalization had taken place nor could we identify any products suggesting that a bis-*N*-oxidation had occurred (by ESI-MS).

Compared to the well-studied optical properties of the Fe(III) complex of tetraphenylporphyrin *N*-oxide,[8,23] the optical properties of the free base of tetraarylporphyrin *N*-oxides have received only scant attention. *N*-Oxidation alters the UV−vis spectrum of porphyrins significantly (Figure 1). As compared to the typical spectrum of a porphyrin, such as **2a**, that is characterized by a sharp Soret band at 418 nm, followed by four side bands in descending intensity, *N*-oxide **3a** possesses a broadened Soret band with a lower extinction coefficient, and the number and relative intensities of the side bands are altered. The longest wavelength absorption ($\lambda_{max}$) is also red shifted by ~40 nm ($\lambda_{max}$ = 686 nm). These effects are likely the result of the nonplanarity of the macrocycle that stems from the steric crowding introduced by the presence of the oxygen atom in the center of the porphyrin. However, the observed UV−vis spectrum could also be influenced by direct electronic effects of the *N*-oxide oxygen.

*N*-Oxides such as **3a** are susceptible to a reversible protonation with TFA.[24] Remarkably, the resulting UV−vis spectrum

(15) W. Poll, W.; Pawelke, G.; Mootz, D.; Appelman, E. H. *Angew. Chem., Int. Ed. Engl.* **1988**, *27*, 392–393.
(16) Posakony, J. J.; Pratt, R. C.; Rettig, S. J.; James, B. R.; Skov, K. A. *Can. J. Chem.* **1999**, *77*, 182–198.
(17) (a) Brückner, C.; Sternberg, E. D.; MacAlpine, J. K.; Rettig, S. J.; Dolphin, D. *J. Am. Chem. Soc.* **1999**, *121*, 2609–2610. (b) Campbell, C. J.; Rusling, J. F.; Brückner, C. *J. Am. Chem. Soc.* **2000**, *122*, 6679–6685. (c) Daniell, H. W.; Brückner, C. *Angew. Chem., Int. Ed.* **2004**, *43*, 1688–1691. (d) McCarthy, J. R.; Hyland, M. A.; Brückner, C. *Org. Biomol. Chem.* **2004**, *2*, 1484–1491.
(18) Brückner, C.; Rettig, S. J.; Dolphin, D. *J. Org. Chem.* **1998**, *63*, 2094–2098.
(19) McCarthy, J. R.; Jenkins, H. A.; Brückner, C. *Org. Lett.* **2003**, *5*, 19–22.
(20) Lara, K. K.; Rinaldo, C. K.; Brückner, C. *Tetrahedron* **2005**, *61*, 2529–2539.
(21) (a) Herrmann, W. A.; Fischer, R. W.; Marz, D. W. *Angew. Chem., Int. Ed. Engl.* **1991**, *30*, 1638–1641. (b) Kühn, F. E.; Scherbaum, A.; Herrmann, W. A. *J. Organomet. Chem.* **2004**, *689*, 4149–4164. (c) Espenson, J. H. *Chem. Commun.* **1999**, 479–488.
(22) Herrmann, W. A.; Kratzer, R. M.; Ding, H.; Thiel, W. R.; Glas, H. *J. Organomet. Chem.* **1998**, *555*, 293–295.
(23) Tsurumaki, H.; Watanabe, Y.; Morishima, I. *Inorg. Chem.* **1994**, *33*, 4186–4188.
(24) HCl, even the traces of HCl present in $CDCl_3$, tend to induce significant decomposition of the *N*-oxide; cf. also to ref 2.

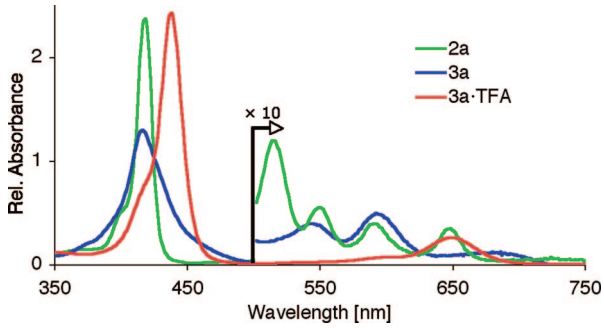


**FIGURE 1.** UV−vis spectra of **2a** (green trace) and **3a** (blue trace) in $CH_2Cl_2$, and **3a**·TFA in $CH_2Cl_2$ + 2% TFA (red trace).

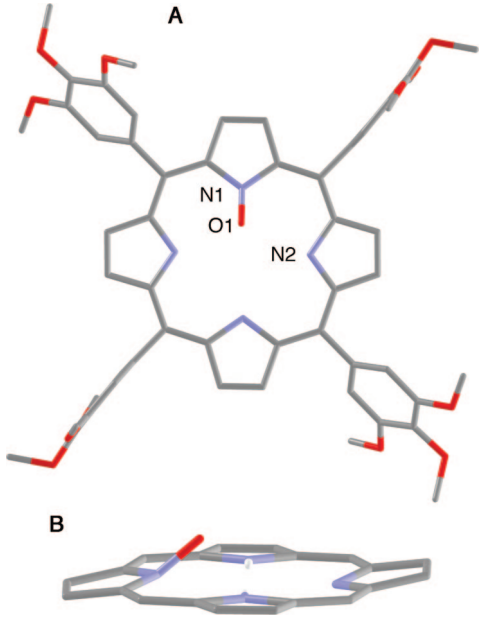


**FIGURE 2.** Stick representation of the single-crystal X-ray structure of **3d**·$CH_2Cl_2$. The disordered solvate $CH_2Cl_2$ H-bound to the *N*-oxide oxygen is not shown. (A) Top view, hydrogen atoms and solvent omitted for clarity. (B) Side view, highlighting the wave-mode distortion of the macrocycle; aryl groups and hydrogens removed for clarity.

of the protonated species **3a**·TFA is virtually identical to that of diprotonated **2a** (for clarity, only the spectrum for protonated **3a** is shown).[25,26] It is well-known that diprotonation induces a severe saddling of the macrocycle.[25] The fact that both **2a**·$2H^+$ and **3a**·TFA possess identical UV−vis spectra appears to indicate that the *N*-oxide moiety has a surprisingly little intrinsic electronic influence on the $\pi$-system of the porphyrin, and most, if not all, changes seen in the UV−vis of **3a** compared to **2a** are due to their conformational differences. As will be demonstrated below, this finding can be largely generalized.

*N*-Oxide **3d** provided crystals suitable for single-crystal X-ray diffractometry, the results of which are shown in Figure 2. The structure, the first for any free base tetraarylporphyrin-derived *N*-oxide, shows the significant out-of-plane displacement of the oxygen atom and the surprisingly minor overall conformational changes the *N*-oxidation has caused. The N−O distance (1.310(10) Å) is somewhat shorter, and the angle of 8.8° at which the oxidized pyrrolic moiety is tipped out of the mean plane formed by the remaining heavy atoms of the macrocycle

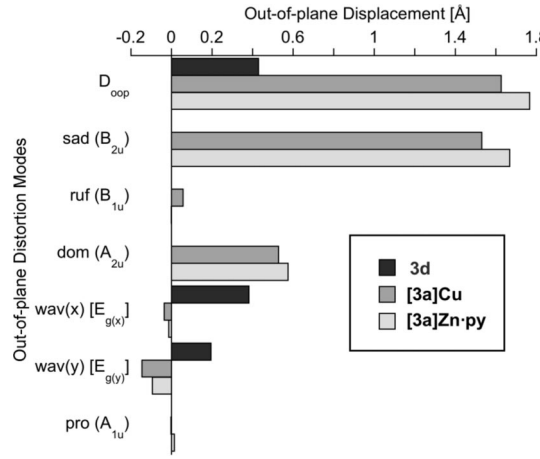


**FIGURE 3.** Lowest-frequency normal-coordinate structural decomposition results for the $C_{20}N_4$ macrocycles of **3d**, and the copper(II) (**[3a]Cu**)[6] and zinc(II)·pyridine complex (**[3a]Zn·py**)[6] of **3a**.

is a little bit larger than observed for the (room temperature) free base OEP *N*-oxide structure (1.398(7) Å and 6.1°, respectively).[3] As in the OEP *N*-oxide—but in contrast to, for example, linear pyridine oxides—the angle between the N−O vector and the plane of the pyrrole to which it is attached is 131° (in OEP *N*-oxide 149.8°). All other features, such as the idealized perpendicular arrangement of the aryl rings with respect to the macrocycle, are entirely as expected.

It is interesting to compare the structure of **3d** to that of a *N*-methylated tetraarylporphyrin.[28] The latter compound is, likely owing to the larger steric bulk of the methyl group, significantly more distorted than **3d**, and for instance, the *N*-methylated pyrrole is tilted 27.7° away from the mean plane of the porphyrin, and the macrocycle is largely deformed in a saddled fashion.[28]

Figure 3 shows the results of a lowest-frequency normal-coordinate structural decomposition (NSD) analysis for the $C_{20}N_4$ macrocycle of **3d** in comparison to that of the copper(II) and zinc(II) complexes of tetraphenylporphyrin *N*-oxide **3a**, thus classifying and quantifying the conformation of the macrocycles.[27] The NSD clearly shows the much smaller overall distortion (as measured as the out-of-plane distortion, $D_{oop}$) of the macrocycle of **3d** compared to the metal complexes. Furthermore, **3d** expresses only the two waving-type distortion modes, whereas the metal complexes also express major saddling and doming components.

In chlorins, the pseudo-olefinic $\beta,\beta'$-double bond that is located opposite of the pyrrolidine moiety is, relatively to the $\beta,\beta'$-bonds in porphyrins, activated.[29] Hence, it might be expected to be more susceptible to a MTO/$H_2O_2$/pyrazole-mediated reaction. Alas, reaction of dimethoxychlorin **4**, made by methylation of the corresponding known diol chlorin,[18] did not generate a bacteriochlorin-like product. Instead, *N*-oxidation

(25) Stone, A.; Fleischer, E. B. *J. Am. Chem. Soc.* **1968**, *90*, 2735–2748.
(26) Brückner, C.; Foss, P. C. D.; Sullivan, J. O.; Pelto, R.; Zeller, M.; Birge, R. R.; Crundwell, G. *Phys. Chem. Chem. Phys.* **2006**, *8*, 2402–2412.

(27) (a) Shelnutt, J. A. In *The Porphyrin Handbook*; Kadish, K. M., Smith, K. M., Guilard, R., Eds.; Academic Press: San Diego, CA, 2000; Vol. 7, pp 167−224. (b) NSD Engine V 3.0: http://jasheln.unm.edu/jasheln/content/nsd/NSDengine/nsd_index.htm (Copyright Lisong Sun, John A. Shelnutt, Sandia National Laboratories).
(28) Lavallee, D. K.; Anderson, O. P. *J. Am. Chem. Soc.* **1982**, *104*, 4707–4708.
(29) See, for example: (a) Brückner, C.; Dolphin, D. *Tetrahedron Lett.* **1995**, *36*, 9425–9428. (b) Berenbaum, M. C.; Akande, S. L.; Bonnett, R.; Kaur, H.; Ioannou, S.; White, R. D.; Winfield, U.-J. *Br. J. Cancer* **1986**, *54*, 717–725. (c) Pandey, R. K.; Shiau, F. Y.; Medforth, C. J.; Dougherty, T. J.; Smith, K. M. *Tetrahedron Lett.* **1990**, *31*, 789–792. (d) Chang, C. G.; Sotiriou, C.; Weishih, W. *J. Chem. Soc., Chem. Commun.* **1986**, 1213–1215.

**SCHEME 2. MTO/$H_2O_2$ Oxidation of *meso*-Tetraphenylchlorins**

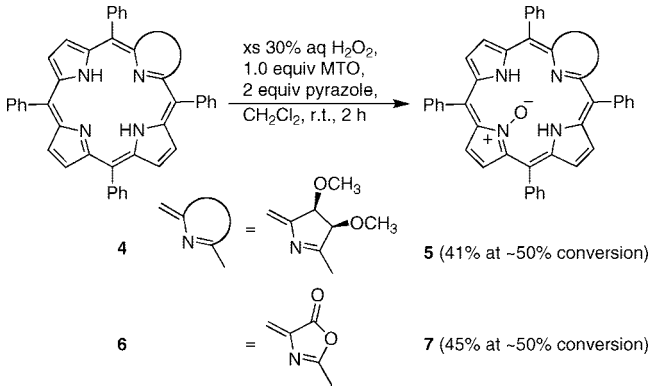


took place forming chlorin *N*-oxide **5**, the first chlorin *N*-oxide described (Scheme 2). The unprotected diol chlorin proved unsuitable for this reactions as it degraded.[30]

As extended reaction times led to an increase in the formation of degradation products, we found it best to allow this, and other reactions (see below), to proceed with stoichiometric quantities of MTO but only to ~50% conversion (TLC control). *N*-Oxide **5** was isolated in 41% yield, and the majority of the remaining starting material could be recovered.

Several diagnostic features in the NMR spectra of **5** place the pyrrole *N*-oxide moiety opposite to the pyrrolidine moiety. The two-fold symmetry of **5** is reflected in the number of signals. Further, the signal assigned to the $\beta$-protons of the pyrrole moiety opposite of the pyrrolidine shifted from 8.53 to 7.43 ppm, indicative for its modification and presumed slanted orientation with respect to the chlorin mean plane and the resulting partial loss of diatropicity. The *cis*-diol functionality differentiates the mean plane of the chlorin into a front side—the side the dimethoxy moiety is pointed toward—and a backside. Hence, we can expect two isomers of **5** (i.e., the isomers in which the *N*-oxide moiety is presented on the front or on the back side). However, we find no indication for the formation of chlorin *N*-oxide isomers. This is either an indication for the selective formation of one isomer or, more likely, presents, as with the findings by Balch and co-workers,[3] another experimental finding for the ability of the *N*-oxide oxygen to swing through the center of the macrocycle. The signals for the $\beta$-protons in the rt $^1$H NMR spectrum ($CD_2Cl_2$) are broadened and do not resolve even at −30 °C into distinct signals.

The UV−vis spectrum of chlorin *N*-oxide **5** is distinctly different from that of the parent chlorin **4** (Figure 4). The distinct chlorin-type side band pattern is lost, and the side bands are broadened in a fashion not unlike that observed for porphyrin *N*-oxide **3a**. Protonation of the *N*-oxide **5** generates a spectrum that is similar compared to the spectrum of protonated chlorin **4** but also shows some distinct differences. Particularly, the split Soret band for **5**·TFA is notable. Thus, here more than simple conformational effects need to be evoked to rationalize the observed UV−vis spectra, but the electronic effects of *N*-oxygenation on the protonated spectra are remarkably small. The protonation event is fully reversible upon addition of a base (e.g., $Et_3N$).

(30) Though an oxidative degradation is assumed, none of the degradation products could be identified as know oxidation product of the diol, such as the corresponding dione (Daniell, H. W.; Williams, S. C.; Jenkins, H. A.; Brückner, C. *Tetrahedron Lett.* **2003**, *44*, 4045–4049) or porpholactone (ref 19).

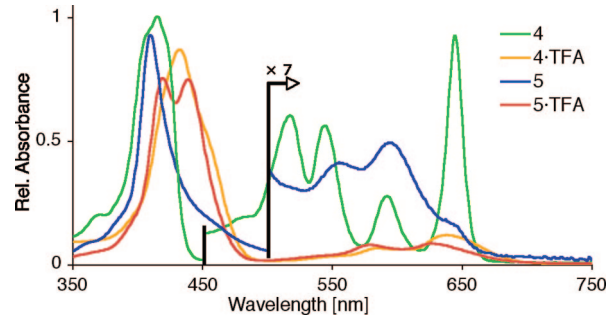


**FIGURE 4.** UV−vis spectra of **4** (green trace) and **5** (blue trace) in $CH_2Cl_2$, and **4**·$2H^+$ (orange trace) and **5**·TFA in $CH_2Cl_2$ + 2% TFA (red trace).

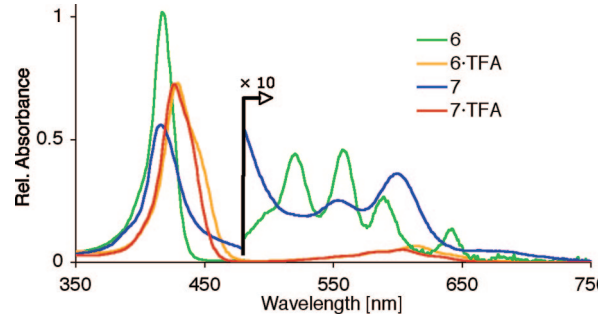


**FIGURE 5.** UV−vis spectra of **6** (green trace) and **7** (blue trace) in $CH_2Cl_2$, and **6**·TFA (orange trace) and **7**·TFA in $CH_2Cl_2$ + 2% TFA (red trace).

Porpholactone **6** is a porphyrinic chromophore in which one $\beta,\beta'$-bond is replaced with a lactone moiety.[31,19] Little is known about its reactivity.[32] When reacted with MTO/$H_2O_2$/pyrazole over the course of 2 h, one major product of higher polarity was formed. The similarity of the changes in the $^1$H NMR spectrum observed with those discussed for the conversion of chlorin **4** to *N*-oxide **5** identified product **7** as the porpholactone *N*-oxide (Scheme 2). Evidently, the directing effect of the oxazolidone moiety with respect to *N*-oxidation is identical to that of a pyrrolidine moiety. Thus, the porpholactone displays here a chlorin-like reactivity.

The UV−vis spectra of porpholactones are very similar to those of porphyrins, but the spectra of the respective protonated species vary (Figure 5).[33] *N*-Oxidation of **6** results in changes in the optical spectra that are reminiscent to those observed for porphyrin **2a**, such as the broadening of the Soret band, reduction of the extinction coefficient by ~50%, and loss of side band features. The effects on the optical properties upon protonation of porpholactone **6** and its *N*-oxide **7** are again remarkably similar, further underlining the minor electronic effects of the *N*-oxide when compared to the effects of the proton-induced conformational changes.

(31) (a) Crossley, M. J.; King, L. G. *J. Chem. Soc., Chem. Commun.* **1984**, 920–922. (b) Gouterman, M.; Hall, R. J.; Khalil, G.-E.; Martin, P. C.; Shankland, E. G.; Cerny, R. L. *J. Am. Chem. Soc.* **1989**, *111*, 3702–3707. (c) Jayaraj, K.; Gold, A.; Austin, R. N.; Ball, L. M.; Terner, J.; Mandon, D.; Weiss, R.; Fischer, J.; DeCian, A.; Bill, E.; Müther, M.; Schünemann, V.; Trautwein, A. X. *Inorg. Chem.* **1997**, *36*, 4555–4566.

(32) Perez, M. J.; McCarthy, J. R.; Brückner, C.; Weissleder, R. *Nano Lett.* **2005**, *5*, 2552–2556.

(33) The protonation of porpholactones takes place in two stages, reflecting the distinctly different $pK_b$s of the two nitrogens; cf. to the observations made for oxypyriporphyrins that also contain a carbonyl group that is in a vinylic position to the nitrogen: Lash, T. D.; Chaney, S. T.; Richter, D. T. *J. Org. Chem.* **1998**, *63*, 9076–9088. At 2% TFA, the diprotonated species of porpholactone is the only species present.

**SCHEME 3. MTO/$H_2O_2$ Oxidation of *meso*-Tetraphenyldithiaporphyrin**

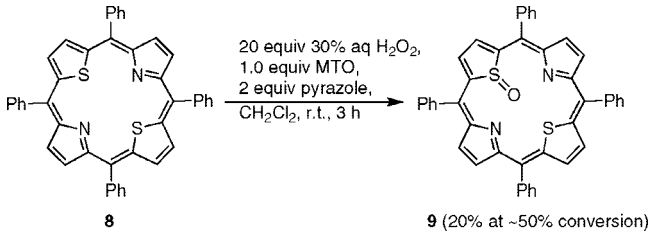


**8** **9** (20% at ~50% conversion)

Heteroporphyrins such as dithiaporphyrin **8** have been well-investigated, but we are not aware of any work that studied their susceptibility to *N*- or *S*-oxidation.[20,34] Submission of **8** to the MTO/pyrazole-mediated $H_2O_2$ oxidation conditions generates a higher polarity product, **9**, albeit in significantly lower yields than the corresponding oxidation of all-aza porphyrins (Scheme 3). Extension of the reaction times or increasing of the stoichiometric ratio of oxidant of catalyst resulted in the formation of a less polar, dark blue side product that we assume, based on its non-porphyrin-like UV−vis spectrum, to be a ring-opened oxidation product. Ultimately, relatively short reaction times and the use of 1 equiv of MTO proved advantageous.

The $^1$H NMR spectrum of **9** indicates that no $\beta,\beta'$-derivatization, such as an epoxidation, had taken place as all four thiophene and pyrrole $\beta$-protons in the aromatic region remained (Figure 6). However, compared to the corresponding signals in porphyrin **8**, each of these, as well as the signals for the *o*-phenyl protons, were split into sets of two, with a splitting pattern (two singlets, 2H each for the thiophene $\beta$-protons and two doublets, 2H each for the pyrrole $\beta$-protons) diagnostic for the formation of a two-fold symmetric molecule, with the (pseudo)-two-fold axis running through both sulfur atoms.

The HR-MS (ESI+, 100% $CH_3CN$) indicates a composition of $C_{44}H_{29}N_2OS_2$ for $\mathbf{9}H^+$ (i.e., the composition expected for the uptake of a single oxygen by dithiaporphyrin **8**). Thus, we assign **9** the structure of hitherto unknown dithiaporphyrin-*S*-oxide. We previously showed that the pyrrolic $\beta$-positions are more reactive toward dihydroxylation reactions using $OsO_4$/pyridine when compared to the thienyl $\beta$-positions.[20] Evidently, here the reactivity of the thiophene sulfur atoms is higher toward oxidation than the reactivity of the pyrrolic nitrogens or any of the $\beta$-positions.

The UV−vis spectrum of sulfoxide **9** is significantly different from that of dithiaporphyrin **8** (Figure 7). The Soret band of **9** possesses only about 1/3 of the extinction coefficient of **8**, is

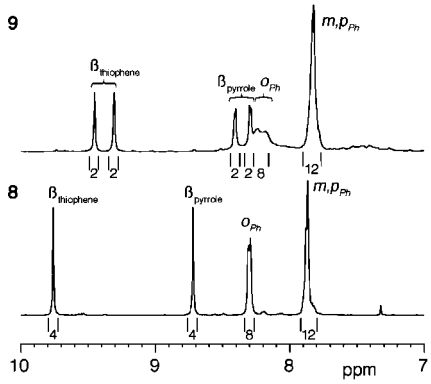


**FIGURE 6.** Aromatic region of the $^1$H NMR (400 MHz, 25 °C) of dithiaporphyrin **8** (bottom; $CD_2Cl_2$) and sulfoxide **9** (top; $CD_2Cl_2$).

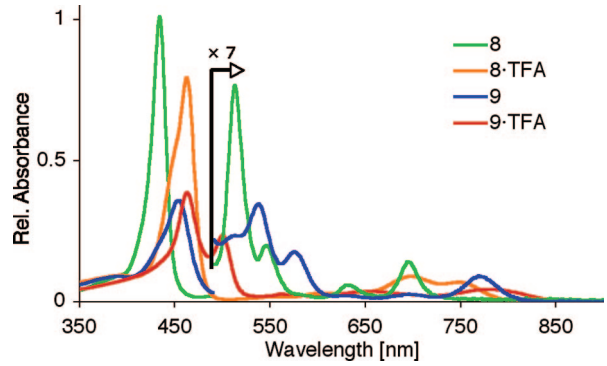


**FIGURE 7.** UV−vis spectra of **8** (green trace) and **9** (blue trace) in $CH_2Cl_2$ and **8**·TFA (orange trace) and **9**·TFA in $CH_2Cl_2$ + 2% TFA (red trace).

**SCHEME 4. MTO/$H_2O_2$ Oxidation of *meso*-Tetratolyl-7,8-*cis*-dimethoxy-21,23-dithiachlorin**

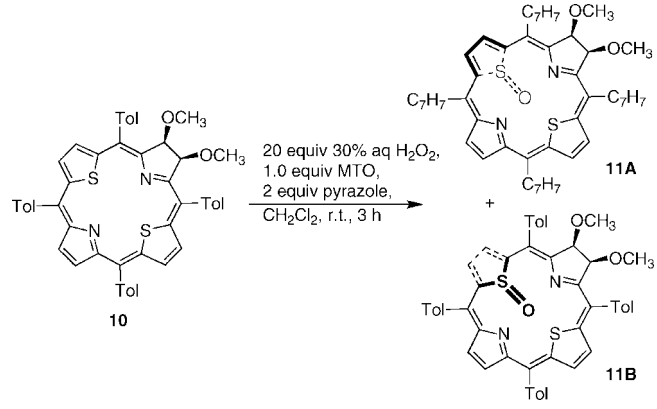


red shifted, and the side bands are significantly broadened and 75 nm red shifted ($\lambda_{max}$ = 769 nm). Thus, the UV data of the S-oxidation product suggest that chromophore **9** is distorted from planarity, but the modulation of the electronic spectrum is distinctly different from that observed upon *N*-oxidation of an all-aza porphyrin (such as **2a**). Moreover, the protonated macrocycles possess very different spectra. Whereas the Soret band of **8**·TFA is red shifted and only marginally broadened, the Soret band of diprotonated **9** is much broadened and split. Of note is also the much red shifted side band for protonated **9** ($\lambda_{max}$ = 778 nm).

We previously reported the dithia-2,3-dimethoxychlorin chromophore.[20] When we exposed this chlorin to the standard MTO/$H_2O_2$/pyrazole conditions, much to our surprise, two compounds of identical UV−vis (see Supporting Information) and composition (as assessed by HR-MS), corresponding to the mono-oxygenated product **11**, were produced in 20% yields each (Scheme 4). Neither product appeared to be very stable or could be prepared in pure form, but the $^1$H NMR spectra of both were interpretable (see Supporting Information). Both NMR spectra are very similar to each other but distinctly different from those of **10** and indicated the presence of compounds lacking any symmetry. Further assuming that chlorin **10** is also susceptible

(34) (a) Ulman, A.; Manassen, J. *J. Am. Chem. Soc.* **1975**, *97*, 6540–6544. (b) Ulman, A.; Manassen, J. *J. Chem. Soc., Perkins Trans. 1* **1979**, *4*, 1066–1069. (c) Stilts, C. E.; Nelen, M. I.; Hilmey, D. G.; Davies, S. R.; Gollnick, S. O.; Oseroff, A. R.; Gibson, S. L.; Hilf, R.; Detty, M. R. *J. Med. Chem.* **2000**, *43*, 2403–2410. (d) Latos-Grazynski, L. In *The Porphyrin Handbook*; Kadish, K. M., Smith, K. M., Guilard, R., Eds.; Academic Press: San Diego, CA, 2000; Vol. 2, pp 361−416.

to *S*-oxidation, the occurrence of two compounds with identical composition and near-identical other spectroscopic properties suggests the formation of the two isomeric *S*-oxides, **11A** and **11B**, that differ by the location of the oxygen—the oxygen resides either on the same side as the two methoxy groups (**11B**) or on the opposite side (**11A**). Both **11A** and **11B** are chiral and are expected to be present as racemic mixtures. The fact that **11** could be separated into these two isomers whereas all-aza chlorin *N*-oxide **5** proved inseparable may be rationalized by the larger steric bulk of the sulfur atoms that does not allow the "swinging through the macrocycle" motion of the oxygen that we evoked to rationalize the absence of isomers in **5**.

In summary, the MTO/pyrazole-mediated $H_2O_2$ oxidation of porphyrins is simple and higher yielding than the traditional methods and mild enough to allow the preparation of chlorin and porpholactone *N*-oxides, the first examples of their class. The solid-state structure of a free base tetraarylporphyrin *N*-oxide shows its intrinsically slightly nonplanar, waved structure. The oxidation of dithiaporphyrin furnishes the corresponding novel *S*-oxide (sulfoxide) that possesses long wavelength absorptions in its UV−vis spectrum. Having now facile access to these chromophores, we are currently testing their reactivity, particularly with respect to their conversion to pyrrole-modified porphyrins.

## Experimental Section

***meso*-Tetraphenylporphyrin-*N*-oxide (3a). General Procedure for the MTO/$H_2O_2$/Pyrazole N-Oxidation of Porphyrins.** In a 50 mL round-bottom flask equipped with a stirring bar, TPP (**2a**) (200 mg, $3.25 \times 10^{-4}$ mol) was dissolved in $CH_2Cl_2$ (20 mL). In a 20 mL scintillation vial with Teflon-lined cap, MTO (20 mg, $8.1 \times 10^{-5}$ mol) suspended in $CH_2Cl_2$ (~1 mL) is mixed with a 30% aqueous $H_2O_2$ solution (750 $\mu$L, $\sim 6.5 \times 10^{-3}$ mmol) by vigorous shaking. The yellow mixture was added at ambient temperature to the vigorously stirring porphyrin solution, followed immediately by pyrazole (44 mg, $6.4 \times 10^{-4}$ mol). When the reaction had proceeded to the desired conversion (~50%, assessed by TLC), the excess $H_2O_2$ was quenched by addition of $MnO_2$ (~50 mg). After stirring for 2 min, the mixture was filtered through a glass frit (M), and the organic layer was separated and dried over $Na_2SO_4$ and reduced by rotary evaporation. The residue was subjected to column (or preparative plate) chromatography (silica, $CH_2Cl_2$/1% MeOH), followed by recrystallization by solvent exchange (with petroleum ether 30−60) on the rotary evaporator. Product **3a** can be isolated in 50−80% yields (100−160 mg): $R_f$ (silica, $CH_2Cl_2$) = 0.19; $^1$H NMR (400 MHz, $CD_2Cl_2$, $\delta$) 9.00 (d, $^3J$ = 4.7 Hz, 2H), 8.85 (d, $^3J$ = 4.7 Hz, 2H), 8.67 (s, 2H), 8.28 (m, 4H), 8.21 (d, $^3J$ = 6.3 Hz, 4H), 7.83−7.73 (m, 12H), 7.55 (s, 2H), 1.07 (br s, exchangeable with $D_2O$, 2H); $^{13}$C NMR (100 MHz, $CD_2Cl_2$, $\delta$) 158.2, 142.8, 141.8, 141.5, 139.4, 139.0, 136.3, 136.0, 135.3, 130.2, 129.7, 128.8, 128.3, 127.7, 127.2, 123.1, 120.3, 120.1; UV−vis ($CH_2Cl_2$) $\lambda_{max}$ [nm] (log $\varepsilon$) 416 (5.21), 544 (3.80), 593 (3.87), 686 (3.39); UV−vis ($CH_2Cl_2$ + 2% TFA) $\lambda_{max}$ [nm] (log $\varepsilon$) 438 (5.48), 594 (sh), 649 (4.48); MS (ESI+, 100% $CH_3CN$, 30 V cone voltage) *m*/*z* 630.7 ($MH^+$); HR-MS (ESI+, 100% $CH_3CN$) calcd for $C_{44}H_{31}N_4O$ ($MH^+$) 631.2498, found 631.2440.

**X-ray Single-Crystal Diffractometry of 3d.** All experimental details, including the cif file, are provided in the Supporting Information.

**Acknowledgment.** We thank Heather W. Daniell, Katherine K. Lara, and Lalith Palitha Samankumara for the preparation of starting materials, and Pedro Daddario for editorial help. This work was supported by the U.S. National Science Foundation under Grant Numbers CHEM-0517782 and CCMI-0730826 (to C.B.). The diffractometer was funded by NSF Grant 0087210, by Ohio Board of Regents Grant CAP-491, and by YSU.

**Supporting Information Available:** All procedures and spectroscopic and analytical data, copies of the $^1$H, $^{13}$C NMR, and FT-IR spectra of the novel compounds, UV−vis spectra of dithiachlorin *S*-oxides **11A** and **11B**, and experimental details to the crystal structure determination of **3d**, including the cif file. This material is available free of charge via the Internet at http://pubs.acs.org.

JO9005443